ChemComm

Design and Synthesis of Capped-Paddlewheel-Based Porous Coordination Cages

SCHOLARONE™
Manuscripts

COMMUNICATION

Design and Synthesis of Capped-Paddlewheel-Based Porous Coordination Cages

Gregory R. Lorzing,[a,b] Eric J. Gosselin,[a] Brian S. Lindner,[a] Rameswar Bhattacharjee,[c] Glenn P. A. Yap,[a] Stavros Caratzoulas,[c] and Eric D. Bloch*[a,b,c]

To leverage the structural diversity of metal-organic frameworks, the ability to controllably terminate them for the isolation of porous coordination cages is advantageous. However, the strategy has largely been limited to ligand termination methods, particularly for paddlewheel-based materials. Here, we show a paddlewheel-capping strategy can be employed to afford previously unattainable coordination cage structures that are mimetic of metal-organic framework pores.

Coordination cages have been widely investigated for a variety of applications including uses in catalysis,[1] biomedicine,[2] separations,[3] and sensing.[4] The discovery of permanent porosity in a subset of these materials has spurred investigations into applications in gas storage,[5] separation,[6] and small-molecule activation.[7] Analogous to record surface area metal-organic frameworks,[8] the highest surface area porous coordination cages are typically based on carboxylic acid ligands and divalent or trivalent metal cations.[9] In fact, many porous cages are essentially molecular analogues of portions of well-known metal-organic frameworks. For these, discrimination between cage and extended structure is achieved by simply terminating a multitopic carboxylate ligand to a lower nuclearity. For example, the reaction of copper(II) with trimesic acid affords a three-dimensional framework whereas reaction with isophthalic acid affords a discrete molecular species.[10,11]

This approach, however, necessarily limits the number of pores within a metal-organic framework that can be isolated as molecular species. This is illustrated for HKUST-1 in Figure 1. The large pore in the material is the isophthalic acid-based $Cu_{24}(bdc)_{24}$ (bdc^{2-} = 1,3-benzenedicarboxylate) cage.[10] Coordination cage analogues of the other pores in the material, which have been implicated as key adsorption sites for gas storage at high pressure,[12,13] are not accessible via this route. These pores are terminated at paddlewheels rather
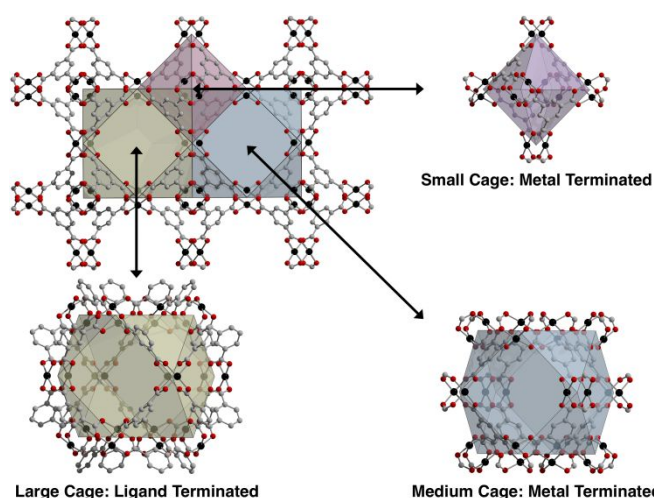

Figure 1. The structure of HKUST-1 (upper left) contains three types of pores. To afford molecular cages the large pore is terminated at the ligand while the other two rely on metal capping units.

than ligands. A cluster capping strategy has previously been successfully employed for a variety of systems to afford, for example, MIL-101,[14] UiO-66,[15] and PCN-9[16] cage analogues by capping with sulfate,[5] cyclopentadienyl,[17] and calixarene,[7,18] respectively. This strategy is particularly challenging for paddlewheel-based cages where cis-divacant coordination sites in starting materials are necessary. Herein we report synthetic routes where either 2,2'-bipyridine or formamidinate ligands are utilized in combination with copper(II) or molybdenum(II) paddlewheels to terminate cluster growth and afford discrete porous cages of trimesic acid.

For this strategy, we initially targeted Mo-based materials given the well-developed coordination chemistry of multiply-bonded Mo_2^{4+} paddlewheel units. Importantly, Cotton *et al.* demonstrated the isolation of an octahedral cage analogous to the small pore in HKUST-1 via the reaction of trimesic acid with $[Mo_2(DAniF)_2(MeCN)_2][BF_4]_2$ (DAniF = N,N'-di-*p*-anisylformamidinate), a Mo-based paddlewheel unit featuring two capping ligands on *cis* coordination sites.[19] The cage, $Mo_{12}(btc)_4(DAniF)_{12}$ (btc^{3-} = 1,3,5-benzenetricarboxylate), features six dimolybdenum paddlewheel units coordinated to four trimesic acid ligands and capped with 12 formamidinate ligands and is directly analogous to the small cage in HKUST-1. Although this molecule is isolable in high yield and features potential porosity, efforts to achieve a porous product via a

[a.] Department of Chemistry and Biochemistry, University of Delaware, Newark, Delaware, 19716, USA. E-mail: edb@udel.edu
[b.] Center for Neutron Science, Department of Chemical and Biomolecular Engineering, University of Delaware, Newark, Delaware, 19716, USA.
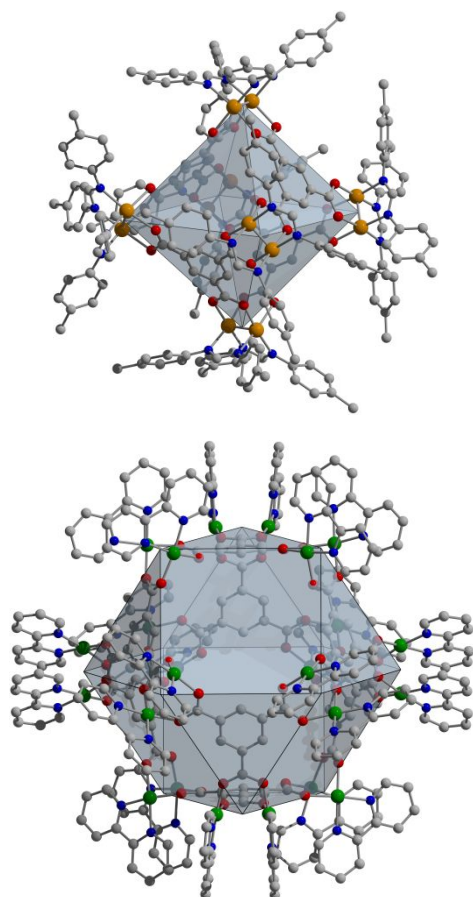[c.] Catalysis Center for Energy Innovation (CCEI) University of Delaware, Newark, Delaware, 19716, USA

Figure 2. (Top) Octahedral $Mo_{12}(btc)_4(DTolF)_{12}$ cage where capping formamidinate ligands coordinate to two metals in an analogous manner to the carboxylate groups. (Bottom) Cuboctahedral $[Cu_{24}(btc)_8(bipy)_{24}]^{24+}$ cage capped with 2,2-bipyridine. Green, orange, red, blue, and grey spheres represent copper, molybdenum, oxygen, nitrogen, and carbon atoms, respectively. Hydrogen atoms, charge balancing perchlorate, and solvent molecules have been omitted for clarity.

variety of crystallization, solvent exchange, and activation methods were unsuccessful. This is likely a result of the interplay of intra- vs. inter-cage porosity.

We have previously shown that small degrees of functionalization of ligands in porous cages can have a profound effect on porosity and gas adsorption properties.[20] Although the carboxylate-based ligands in Cotton's cage lack sites accessible to straightforward functionalization, the capping formamidinate ligands are highly tunable. For these, the reaction of triethylorthoformate with 4-functionalized aniline derivatives affords capping ligands, coincident with release of ethanol, in high yield. We adopted a slightly modified procedure to produce $M_{12}btc_4L_{12}$ cages based on tolyl-functionalized caps. Here, the reaction of molybdenum hexacarbonyl with N,N'-di-*p*-tolylformamidinate (HDTolF) in orthodichlorobenzene affords $Mo_2(DTolF)_4$ in quantitative yield. Reaction of this paddlewheel with six equivalents of trimethyloxonium tetrafluoroborate in acetonitrile (MeCN) selectively oxidizes *cis* paddlewheel ligands to afford $Mo_2(DTolF)_2(MeCN)_4^{2+}$. This bimetallic unit featuring coordinating acetonitrile ligands further reacts with btc^{3-} in MeCN to afford the octahedral cage $Mo_{12}(btc)_4(DTolF)_{12}$ as determined by single-crystal X-ray diffraction (Figure 2). The quadruply bonded bimetallic units in this cage feature Mo–Mo bonds of 2.09 Å and reside at the vertices of the octahedron

with paddlewheel-paddlewheel distances of ~10 Å. The cages pack in the solid state with cage center–center distances of approximately 20 Å. Close inspection of the crystal structure of this compound reveals significant solvent-accessible voids. Accordingly, thermogravimetric analysis (TGA) of a recrystallized sample shows a mass loss of 20 % by 150 °C. It noteworthy that the medium pore in HKUST-1 contains the identical 3:1:3 metal:ligand:cap ratio as this small octahedral cage. However, our attempts to isolate this species, $Mo_{24}(btc)_8(DTolF)_{24}$, as a molecular cage were unsuccessful regardless of reaction conditions. Tuning the donating strength of the capping formamidinate ligand may be a viable strategy for isolating the higher nunclearity cage, which is the thermodynamically less favoured product.

To achieve appreciable surface areas for porous cages, great care must be taken with solvent exchange and removal. Coordination cages are potentially soluble in many organic solvents, limiting the number of these accessible for exchange. Similarly, as porous cages lack three-dimensional connectivity, lower activation temperatures are often required. For $Mo_{12}(btc)_4(DTolF)_{12}$, recrystallization from CH_2Cl_2 via MeCN layering, followed by thorough MeCN exchanges and room temperature activation resulted in an optimal surface area. The cage displays a BET (Langmuir) surface area of 446 (547) m^2/g as determined from N_2 adsorption at 77 K. Pore-size distribution calculations indicate the octahedral cage in the material is the most prevalent pore, with additional porosity ascribed to pore-space extrinsic to the octahedral cage. The coordination cage displays appreciable solubility in a variety of organic solvents, including N,N-dimethylformamide (DMF), chloroform, and methylene chloride. The utility of a porous molecular material is illustrated by rapidly removing solvent from a CH_2Cl_2-dissolved sample which affords a material with a Langmuir surface area of 507 m^2/g.

We expect this formamidinate-capping strategy to be widely applicable to isolate porous molecular analogues of a variety of metal-organic framework pores based on second-row metals. For the isolation of cages based on first-row metals, however, a significantly altered strategy must be employed. This is a result of relative difficulty in preparing not only formamidinate-based paddlewheel units, but mixed carboxylate/formamidinate paddlewheels with first-row metals. The few reported examples of these have been limited to chromium(II).[21] Additionally, it is difficult to discriminate between *cis*- and *trans*-formamidinate capping in these systems. This is avoidable with the use of ligands where *cis*-coordination is enforced by bidentate ligands such as bipyridine or phenanthroline. A library of such coordination complexes has been reported for copper(II) paddlewheels. For these, two carboxylate ligands (typically acetate) bridge two copper(II) cations while bipyridine ligands coordinate to the two remaining paddlewheel coordination sites.[22] Analogous to the liberation of coordinated acetonitrile upon reaction of $Mo_2(DTolF)_2(MeCN)_4^{2+}$ with trimesic acid, the acetate ligands of bipyridine or functionalized bipyridine capped copper paddlewheels can be selectively removed upon reaction with a multitopic carboxylic acid ligand.

Here, the reaction of 2,2'bipyridine capped copper acetate, $Cu_2(OAc)_2(bipy)_2[ClO_4]_2$,[23] with H_3btc in methanol at room temperature affords a teal-blue powder in high yield (*Caution!-transition metal perchlorate salts are potentially explosive, particularly when anhydrous*). Diffraction-quality single crystals
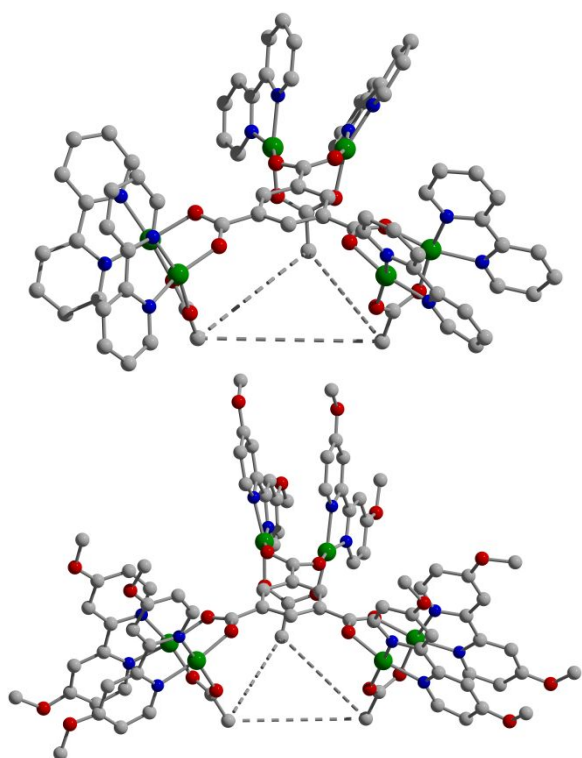
Figure 3. Optimized broken-symmetry structures for $[Cu_6(bipy)_6(OAc)_3(btc)]^{6+}$ (top) and $[Cu_6(OMe-bipy)_6(OAc)_3(btc)]^{6+}$ (bottom). The steric effect of the –methoxy groups on the latter decreases the $RCOO^-_{btc}$–$RCOO^-_{OAc}$ angle and drives assembly toward the small cage. The average $C_{acetate}$–$C_{acetate}$ distance depicted in the top structure is 7.94 Å as compared to 7.53 Å in the methoxy-functionalized cluster.

of this material were prepared via slow evaporation of a saturated acetonitrile solution at room temperature. Structural determination reveals the cage does not adopt a structure analogous to $Mo_{12}(btc)_4(DToIF)_{12}$. Rather, this copper cage $[Cu_{24}(btc)_8(bipy)_{24}][ClO_4]_{24}$ adopts a cuboctahedral structure with eight triangular windows and six square windows. The cage consists of twelve dicopper paddlewheel units coordinated to eight btc^{3-} ligands on every triangular window (Figure 2). The square windows feature metal-bound perchlorate or solvent molecules at the axial sites of the copper paddlewheels. In this cage, the bipy capping ligands remain on the paddlewheel with one 2,2'-bipyridine coordinated to *cis* sites on each copper(II). This cage is conceptually similar to the previously reported isophthalic acid-based cuboctahedral cage $Cu_{24}(bdc)_{24}$.[10] The paddlewheel-paddlewheel distances are slightly shorter in the bipy-capped cage with distances of approximately 9.21 Å along the edges of the square and triangular windows, as compared to 9.35 Å in $Cu_{24}(bdc)_{24}$. As a result of this, the paddlewheel-paddlewheel distance of 18.54 Å across the cage is slightly shorter than the distance in the isopthalic acid cage (18.69 Å). Although $[Cu_{24}(btc)_8(bipy)_{24}][ClO_4]_{24}$ displays negligible N_2 accessible surface area, fits to a CO_2 isotherm collected at 195 K on a sample activated at 100 °C reveals a BET (Langmuir) surface area of 104 (334) m^2/g. The inaccessibility of the structure to N_2 at 77 K is likely a result of pore blockage from copper-coordinated charge balancing perchlorate. However, the surface area is similar to the BET value of 248 m^2/g reported for $Cu_{24}(bdc)_{24}$.[24]

Although it is expected that the lower nuclearity octahedral cage should be isolable under similar conditions

that afforded the cuboctahedral structure, we were unable to isolate this material under any synthetic conditions that were attempted. As ligand functionalization can be used to control phase in both MOFs and coordination cages, we turned to computational methods to give insights into design criteria that would allow for the tunable control of cage phase. Similar to the 4-position ligand functionalization to control crystal packing in the Mo^{2+} cage, we investigated 4- and 5-functionalization of 2,2'-bipyridine. Here we utilized a 6-metal/1-btc portion of the cage shown in Figure 3 that is terminated with acetate ligands. Structure optimization of the unfunctionalized cluster and a 4,4'-dimethoxy-functionalized bipy ligand at the M06-L/6-31G(d,p) level show the methoxy groups are sufficient to tune the spacing between acetate carbon atoms in the cluster, with an average C–C distance of 7.94 Å in the unfunctionalized structure and 7.53 Å in the methoxy-functionalized structure (Figure 3). Further, these calculations suggest no appreciable differences in the electronic structure of the copper ions in each cluster.

Indeed, the reaction of a 4,4'-dimethoxy-functionalized bipyridine-capped paddlewheel, $Cu_2(OAc)_2(OMe-bipy)_2[ClO_4]_2$ with H_3btc in methanol at room temperature affords a teal-blue powder in high yield. Diffraction-quality single crystals of this material were prepared via layering of diethyl ether on a saturated acetonitrile solution at 8 °C. Structural determination reveals the cage indeed adopts a structure analogous to $Mo_{12}(btc)_4(DToIF)_{12}$. This copper cage, $[Cu_{12}(btc)_4(OMe-bipy)_{12}][ClO_4]_{12}$, similarly features six dicopper paddlewheel units in an octahedral arrangement coordinated to four btc^{3-} ligands on four of the faces of the cage (Figure 4). As expected based on the computational model, the $C_{carboxylate}$–$C_{carboxylate}$ distances analogous to those shown in Figure 3 are approximately 7.65 Å and the methoxy groups are indeed incompatible with the close proximity enforced by the larger cuboctahedral cage. The paddlewheel-paddlewheel distance of ~13.2 Å is slightly shorter than the distance of 13.5 Å in the molybdenum cage. This is likely partially a result of the chelating nature of bipy, which displays significantly decreased N–Cu–N angles of ~82° as compared to N–Mo–N angles of approximately 97° for the formamidinate-capped cage. This causes the trimesic acid ligands of the copper species to pucker significantly, decreasing the size of the cage. A CO_2
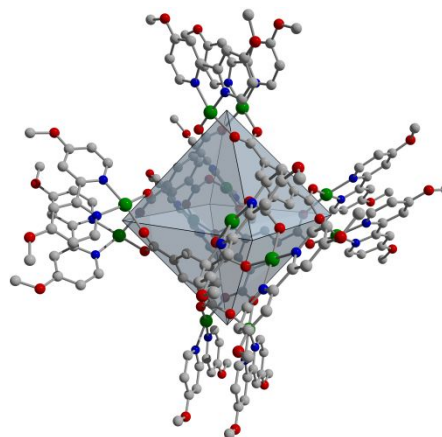

Figure 4. Octahedral $[Cu_{12}(btc)_4(OMe-bipy)_{12}]^{12+}$ where the bipyidine caps coordinate to *cis* sites on a single copper center and feature *pi-pi* stacking with the bipy ligand on the adjacent copper. Green, red, blue, and grey spheres represent copper, oxygen, nitrogen, and carbon atoms, respectively. Hydrogen atoms, perchlorate ions, and solvent molecules have been omitted for clarity.

isotherm collected at 195 K reveals a BET (Langmuir) surface area of 151 (362) m^2/g for this material upon activation at 100 °C. Pore-size distribution calculations reveal a majority of the surface area is attributable to 12.6 and 18.1 Å pores.

In contrast to the Mo-based cage, neither the octahedral nor cuboctahedral copper cages display measurable surface areas upon rapid evacuation of solvent from acetonitrile solutions. In this case, both $[Cu_{24}(btc)_8(bipy)_{24}][ClO_4]_{24}$ and $[Cu_{12}(btc)_4(OMe\text{-}bipy)_{12}][ClO_4]_{12}$ have CO_2 accessible surface areas that are less than 10 m^2/g. However, we envision that his property can be tuned by utilizing ligand functionalization to tune density, and thus volumetric storage capacity, in designer cages. Further, it is expected that utilization of porous counter anions with these porous cationic cages will be a viable route to tune porosity and gas uptake properties.

The aforementioned results illustrate how the judicious utilization of capping ligands in paddlewheel systems can afford porous coordination cages analogous to metal-terminated pores in metal-organic frameworks. For metal cations amenable to cis-divacant coordination sites, such as molybdenum(II), formamidinate-type ligands can potentially be incorporated into porous cages. Bipyridine-based capping ligands can be used with first-row metals in order to isolate novel paddlewheel-based cages. We envision the strategies outlined here can be widely applied to a variety of first- and second-row transition metals and numerous carboxylate-based multitopic organic ligands. Future work in our lab along these lines will focus on preparing copper(II) and chromium(II) materials with a variety of anions for gas storage and separation applications.

Conflicts of interest

There are no conflicts to declare.

References

1   T. Murase, Y. Nishijima, M. Fujita, *J. Am. Chem. Soc.*, 2012, **134**, 162-164; W. Cullen, A. J. Metherell, A. B. Wragg, C. G. P. Taylor, N. H. Williams, M. D. Ward, *J. Am. Chem. Soc.*, 2018, **140**, 2821-2828;

2   V. Vajpayee, Y. H. Song, Y. J. Yang, S. C. Kang, T. R. Cook, D. W. Kim, M. S. Lah, I. S. Kim, M. Wang, P. J. Stang, K.-W. Chi, *Organometallics*, 2011, **30**, 6482-6489; T. R. Cook, V. Vajpayee, M. H. Lee, P. J. Stang, K. -W. Chi, *Acc. Chem. Res.*, 2013, **46**, 2464-2474.

3   M. Han, R. Michel, B. He, Y. -S. Chen, D. Stalke, M. John, G. H. Clever, *Angew. Chem. Int. Ed.*, 2013, **52**, 1319-1323; W. Xuan, M. Zhang, Y. Liu, Z. Chen, Y. Cui, *J. Am. Chem. Soc.*, 2012, **134**, 6904-6907.

4   S. J. Lee, W. Lin, *J. Am. Chem. Soc.*, 2002, **124**, 4554-4555; A. Kumar, S. -S. Sun, A, J. Lees, *Coord. Chem. Rev.*, 2008, **252**, 922-939.

5   A. C. Sudik, A. R. Millward, N. W. Ockwig, A. P. Cote, J. Kim, O. M. Yaghi, *J. Am. Chem. Soc.*, 2005, **127**, 7110-7118.

6   E. V. Perez, K. J. Balkus, J. P. Ferraris, I. H. Musselman, *J. Memb, Sci.*, 2014, **463**, 82-93; J. Park, L. -B. Sun, Y. -P. Chen, Z. Perry, H. -C. Zhou, *Angew. Chem. Int. Ed.*, 2014, **53**, 5842-5846.

7   Y. Fang, Z. Xiao, J. Li, C. Lollar, L. Liu, X. Lian, S. Yuan, X. Banerjee, P. Zhang, H. -C. Zhou, *Angew. Chem. Int. Ed.*, 2018, **57**, 5283-5287.

8   O. K. Farha, I. Eryazici, N. C. Jeong, B. G. Hauser, C. E. Wilmer, A. A. Sarjeant, R. Q. Snurr, S. T. Nguyen, A. O. Yazaydin, J. T. Hupp, *J. Am. Chem. Soc.*, 2012, **134**, 15016-15021.

9   Z. Ju, G. Liu, Y.-S. Chen, D. Yuan, B. Chen, *Chem. Eur. J.*, 2017, **23**, 4774-4777.

10 M. Eddaoudi, J. Kim, J. B. Wachter, H. K. Chae, M. O'Keeffe, O. M. Yaghi, *J. Am. Chem. Soc.*, 2001, **123**, 4368-4369; B. Moulton, J. Lu, A. Mondal, M. J. Zaworotko, *Chem. Commun.*, 2001, 863-864.

11 M. Kramer, U. Schwarz, S. Kaskel, *J. Mater. Chem.*, 2006, **16**, 2245-2248; L. Xie, S. Liu, C. Gao, R. Cao, J. Cao, C. Sun, Z. Su, *Inorg. Chem.*, 2007, **46**, 7782; L. J. Murray, M. Dinca, J. Yano, S. Chavan, S. Bordiga, C. M. Brown, J. R. Long, *J. Am. Chem. Soc.*, 2010, **132**, 7856-7857; P. Maniam, N. Stock, *Inorg. Chem.*, 2011, **50**, 5085; O. Kozachuk, K. Yusenko, H. Noei, Y. Wang, S. Walleck, T. Glaser, R. A. Fischer, *Chem. Commun.*, 2011, **47**, 8509-8511; Z. Zhang, L. Zhang, L. Wojtas, M. Eddaoudi, M. J. Zaworotko, *J. Am. Chem. Soc.* 2012, **134**, 928-933.

12 Z. Hulvey, B. Vlaisavljevich, J. A. Mason, E. Tsivion, T. P. Dougherty, E. D. Bloch, M. Head-Gordon, B. Smit, J. R. Long, C. M. Brown, *J. Am. Chem. Soc.* 2015, **137**, 10816-10825.

13 Z. Hulvey, K. V. Lawler, Z. Qiao, J. Zhou, D. Fairen-Jimenez, R. Q. Snurr, S. V. Ushakov, A. Navrotsky, C. M. Brown, P. M. Forster, *J. Phys. Chem. C*, 2013, **117**, 20116-20126.

14   P. L. Llewellyn, S. Bourrelly, C. Serre, A. Vimont, M. Datury, L. Hamon, G. D. Weireld, J. -S. Chang, D. -Y. Hong, Y. K. Hwang, S. H. Jung, G. Ferey, *Langmuir*, 2008, **24**, 7245-7250.

15 J. H. Cavka, S. Jakobsen, U. Olsbye, N. Guillou, C. Lamberti, S. Bordiga, K. P. Lillerud, *J. Am. Chem. Soc.*, 2008, **130**, 13850-13851.

16 S. Ma, H.-C. Zhou, *J. Am. Chem. Soc.*, 2006, **128**, 11734-11735.

17 G. Liu, Z. Ju, D. Yuan, M. Hong, *Inorg. Chem.*, 2013, **52**, 13815-13817; D. Nam, J. Huh, J. Lee, J. H. Kwak, H. Y. Jeong, K. Choi, W. Choe, *Chem. Sci.*, 2017, **8**, 7765-7771.

18 Y. Fang, J. Li, T. Togo, F. Jin, Z. Xiao, L. Liu, H. Drake, X. Lian, H. -C. Zhou, *Cell*, 2018, **4**, 555-563.

19 F. A. Cotton, L. M. Daniels, C. Lin, C. A. Murillo, *Chem. Commun.*, 1999, 841-842.

20 O. Barreda, G. Bannwart, G. P. A. Yap, E. D. Bloch, *ACS Appl. Mater. Interfaces*, 2018, **10,** 11420-11424.

21 F. A. Cotton, L. M. Daniels, C. A. Murillo, P. Schooler, *J. Chem. Soc., Dalton Trans.*, 2000, 2001-2005; F. A. Cotton, Z. Li.,C. A. Murillo, *Eur. J. Inorg. Chem.*, 2007, 3509-3513.

22 S. P. Perlepes, J. C. Huffman, G. Christou, *Polyhedron*, 1992, **11**, 1471-1479.

23 M. Toofan, A. Boushehri, M. Ul-Haque, *J. Chem. Soc., Dalton Trans.,* 1976, **0**, 217-219.

24 J. Yang, M. Lutz, A. Grzech, F. M. Mulder, T. J. Dingemans, *CrystEngComm*, 2014, **16**, 5121-5127.